Concept study for a compact planetary homodyne interferometer (PHI) for temporal global observation of methane on Mars in IR

Sona Hosseini*[a], Chris Webster[a], Geoffrey Toon[a], Wesley Traub[a], John Trauger[a]
[a]Jet Propulsion Labratory, California Institute of Technology, Pasadena, California 91109, USA

ABSTRACT

We present a concept study to develop a new instrument to sequentially and over a long time measure methane abundance on Mars and find out its global seasonal variations, if any. The ***Planetary Homodyne Interferometer (PHI)*** can offer integrated spectra over a wide field-of-view (FOV) in high spectral resolution (R~10^5) in a compact design using no (or a small < 1m) primary mirror. PHI is best suited to studies of sources where temporally tracing specific spectral features sensitivity, and spectral resolution is of higher significance than spatial fidelity.

Keywords: Mars, methane, Spatial Homodyne Spectrometer, SHS, extended targets, interferometry, spectrometry,

1. INTRODUCTION

Here we describe the study for a new compact, high-performance, high spectral resolution Infrared (IR) spectrometer for Mars atmospheric methane measurement from space-based platforms. Methane has been detected in the atmosphere of Mars using different approaches from in situ measurement by Curiosity, ground-based telescopic observations, and remote-sensing measurements from Mars-orbiting spacecraft MEX, MGS, and MRO. Although each approach has reported various results, these results cannot be contradictory, due to the possibility of spatial and temporal variability. We present a concept study to build a new instrument to sequentially and over a long time measure methane abundance on Mars and find out its global seasonal variations, if any. The ***Planetary Homodyne Interferometer (PHI)*** offers integrated spectra over a wide field-of-view (FOV) in high spectral resolution (R~10^5) in a compact design using no (or a small < 1m) primary mirror. The architecture of PHI combines the high étendue of a Fourier Transform Spectrometer with higher optomechanical tolerance and simpler optomechanical design associated with grating spectrometers. We are targeting to measure the mid-infrared absorption of Mars atmospheric CH_4, H_2O, and CO_2 absorption lines by observing the full disk of Mars from Mars's orbit.

2. SCIENTIFIC OBJECTIVES OF MARS METHANE OBSERVATIONS

Methane has been detected in the atmosphere of Mars using 3 different approaches: in situ measurement at Gale Crater from Curiosity [1, 2], ground-based telescopic observations[3], and remote-sensing measurements from Mars orbiting spacecraft MEX [4], MGS [5] and MRO [6]. Earth's atmospheric methane is predominantly biologically-produced. Determining the abundance and variability of methane in the current Martian atmosphere is critical to assessing the contribution from a variety of potential sources or reservoirs that may be biological or abiotic. These latter processes include: geological production such as serpentinization of olivine, UV degradation of meteoritically-delivered organics, production by impacts of comets, release from subsurface clathrates or regolith-adsorbed gas, erosion of basalt with methane inclusions, or geothermal production.

Several detections of Mars methane have been published. Ground-based observations from the Canada-France-Hawaii Telescope (CFHT) in 1999 found a global average value of 10±3 ppbv, and those using the NASA IRTF telescope in 2003 reported [3] methane in plumes from discrete sources in Terra Sabae, Nili Fossae, and Syrtis Major that showed seasonal changes with a summer time maximum of ~45 ppbv near the equator. The Planetary Fourier Spectrometer (PFS) on the Mars Express (MEX) spacecraft reported detection in 2004 with an updated global average abundance of 15±5 ppbv [4], with indications of discrete localized sources and a summer time maximum of 45 ppbv in the north polar region. From the Thermal Emission Spectrometer (TES) of Mars Global Surveyor (MGS), methane abundances from 5 to 60 ppbv were

deduced [5] as intermittently present over locations where favorable geological conditions such as residual geothermal activity (Tharsis and Elysium) and strong hydration (Arabia Terrae) might be expected. Using data from NASA-IRTF acquired in February 2006, reference [3] reported a detection of 10 ppbv at mid-latitudes (42-7°N) over Valles Marineris but an upper limit of 3 ppbv outside that region; in December 2009 they obtained an upper limit of 7-8ppbv.

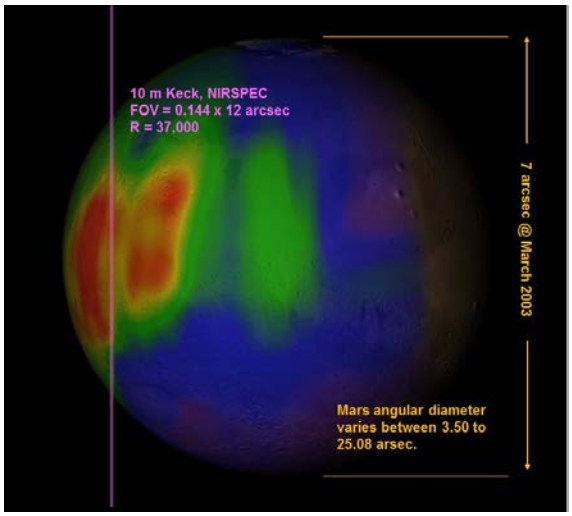

Figure 1. Global Mars methane map produced by Mumma et al. [4], with the magenta pink lines representing the FOV of the Keck telescope instruments. Mumma et al. had a small FOV, and needed to produce a single map with hundreds of 30-min observations over a 5-day period in March 2003. PHI could identify methane by looking at the entire planet in one shot in a short time in any time of the year and map seasonal changes with time.

Observational evidence for methane on Mars has been questioned in the published literature [7] because photochemical models are unable to reconcile the observed amounts with their reported spatial gradients and temporal changes over months compared with the expected ~300 year methane lifetime [8]. Contradictions were noted between the locations of maxima reported from ground-based observations and maps inferred by PFS and TES from Mars orbit. The plume results were questioned on the basis of a possible misinterpretation from methane lines whose positions coincided with those of terrestrial isotopic $^{13}CH_4$ lines. Model calculations including expected atmospheric transport and circulation are to date all unable to reproduce the spatial and temporal characteristics of the observed high concentration methane plumes, despite the introduction of a variety of putative loss mechanisms.

The Tunable Laser Spectrometer (TLS) of the Sample Analysis at Mars (SAM) instrument suite on Curiosity rover has a spectral resolution of R=27,000,000 at 0.0002 cm^{-1} that offers unambiguous identification of methane in a unique fingerprint spectral pattern of 3 well-resolved adjacent $^{12}CH_4$ lines in the 3.3-µm band , scanning across seven rotational lines that includes the R(3) triplet used in this study. The Curiosity team reported [1] measurement of the background levels of methane at 0.7 ±0.2 ppbv, and observation of an episodic release at levels ten times this value.

Although the Curiosity measurements can be understood without the need to invoke new chemistry or processes within the Martian atmosphere, the earlier Mumma et al. [3] measurements are puzzling and certainly require faster loss mechanisms that would reduce the methane lifetime appropriately. The community consensus is that more measurements are needed to reconcile the ground-based, orbiter and rover results, and to reveal the underlying processes, sources and sinks that drive the observed abundance, its distribution, and temporal behavior. Specifically, a measurement sensitivity of 1 ppbv or less is required to make progress in understanding the Mars methane mystery.

3. THE PHI INSTRUMENT CONCEPT

PHI is a concept study to sequentially and over a long time measure methane abundance on Mars and find out its global seasonal variations in large scale, if any. The ***Planetary Homodyne Interferometer (PHI)*** can offer integrated spectra over a wide field-of-view (FOV) in high spectral resolution (R~10^5) in a compact design using no (or a small < 1m) primary

mirror, from Earth's orbit, Mars' orbit or from a lander on Mars. The architecture of PHI combines the high étendue of a Fourier Transform Spectrometer with higher optomechanical tolerance and simpler optomechanical design associated with grating spectrometers.

Accounting for multiple scattering is achieved by simultaneously measuring other gases in the same wavelength range such as CO_2, the dominant Martian atmospheric molecule, which provides an air mass along the same effective absorption path length through the atmosphere. These global measurements will add to the observations to date, and be able to resolve questions to date concerning the exact abundances, their vertical extent and seasonal variations.

3.1 PHI Optical Design

PHI is a compact two-beam interferometer that produces a 2-D Fizeau fringe pattern from which the input spectrum can be obtained via a Fourier transform. The basic PHI is based on a reflective SHS design [9-11] and similar to a non-scanning FTS device that combines high resolving power and a large input acceptance angle in a compact format. Earlier SHS instrument designs were of a Michelson interferometer in which the mirror in each interferometer arm was replaced by a grating [11, 12], subsequently adapted for remote sensing applications through the incorporation of a two-dimensional camera CCD detector that captured the instrumental bandpass into a self-scanned image [11, 13-15]. This led to a series of ground and space-based Michelson design SHS instruments for observations of atmospheric and interstellar emission line features [15, 16]. Parallel to US groups, there also have been European efforts to develop SHS for use with the next generation of large aperture telescopes [17]. To date, the majority of the SHS projects are in the Michelson SHS format. A major weakness of Michelson SHS instruments is their use of transmitting elements (beam splitter), which limits their usefulness in shorter wavelengths (UV).

PHI is a cyclical interferometer where the two beams travel a *common path* in opposite directions through the interferometer (similar to a Sagnac Interferometer). In reflective SHS (figure 2) the grating diffracts an incoming collimated beam into ±m orders following the grating equation for normal incidence $[\sin\beta_{in} + \sin\beta_{out}]\cos\Theta = mG\lambda$, where λ is the wavelength, G is the groove spacing density and Φ is the diffraction angle relative to the grating normal. After division, the two beams anti-symmetrically traverse the optical path, converge back at the grating, and then exit from the system. To separate the incoming and outgoing beams, one of the transfer mirrors is replaced by a right angle 'roof' mirror that translates both beams down to a parallel plane below (or above) the incoming optical path. For the tuned wavelength λ_0, called the homodyne wavelength, the optics are aligned such that the two beams return to the grating with the same angle as the original diffraction, so they will overlap at the grating and exit parallel to the incoming beam and each other and

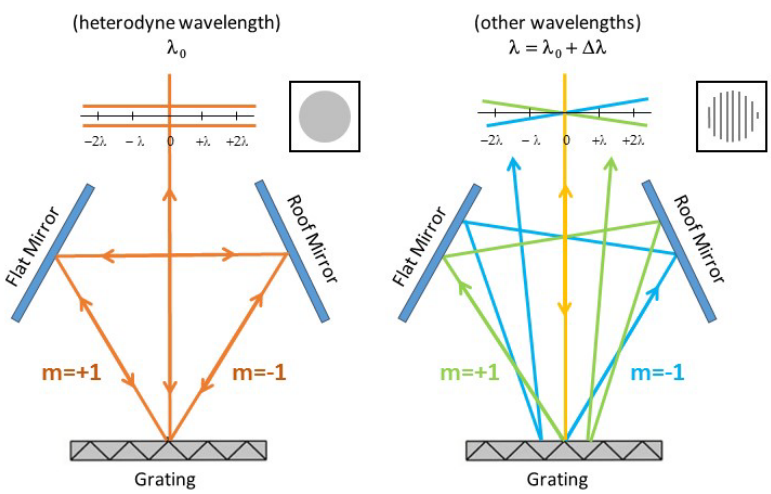

Figure. 2 (Left) PHI is based on a simple cyclical design. The incoming collimated light hits the grating at normal incident, splits to two orders, travel in opposite directions, and diffract off the grating before exiting. For the tuned wavelength λ_0 everything is symmetric, there is no path or phase differences between the emerging beams. **(Right)** However the exiting wave fronts of other wavelengths ($\lambda=\lambda_0+\Delta\lambda$) are tilted in respect to each other producing a fringe pattern.

hence create no fringes [10]. This case is referred to as the 'homodyne condition'. At all other wavelengths ($\lambda=\lambda_0+\Delta\lambda$) there is a dispersive rotation introduced to the merging wave fronts by the gratings that directs the two beams in slightly different outgoing directions. This tilt results in the formation of a 2-D Fizeau fringes with a frequency dependent on $\Delta\lambda$ [10]. The Fourier transform of the fringe pattern recovers the original power spectrum in units of wavelength separation from λ_0. Alignment of PHI involves the rotation of one or both of the transfer mirrors to set the angles such that a chosen wavelength satisfies the homodyne condition (λ_0) [10, 18].

3.2 PHI Fringe localization plane and data collecting

The data fringe pattern forms at a location called the *Fringe Localization Plane* (*FLP*) and is imaged onto an imaging 2-D detector [10]. *FLP* is defined by following the diverging exiting beams from the interferometer, and is a virtual plane located at distance z_0 behind the grating on the z-axis [19]. For a complex spectrum, each wavelength diffracts in different angle, resulting in a superposition of fringes in different frequencies and intensities. The Fourier transform of the interference pattern imaged onto the detector recovers the power spectrum of the input light. At small angle approximation [10] $z_0 \sim L/2\cos^2\beta_0$ where L is the average optical path inside PHI and β_0 is the first diffraction angle of the homodyne wavelength λ_0 . The recorded interference pattern on the detector at wavenumber σ is defined as:

$$I(\mathrm{x},\mathrm{y},\mathrm{z}_0,\sigma)=\int_{\sigma_1}^{\sigma} I(\sigma)\,d\sigma\left[1+\cos\left(2\pi\left(f_x\,x+f_y\,y+f_z\,z_0\right)\right)\right]$$

in which

$$f_x \approx -4\,\delta\sigma\sin\beta_0$$
$$f_y \approx 2\,\sigma\,\phi$$
$$f_z \approx 2\sigma\sqrt{1-4\sin\beta_0^2\left(\frac{\delta\sigma}{\sigma}\right)^2}$$

where $I(\sigma)$ is the spectral intensity of the input light, σ_1 and σ_2 define the bandpass boundary in wavenumber and ϕ is the cross tilt in the mirrors perpendicular to the grating diffraction plane [10, 11, 20]. For a complex spectrum, each different wavenumber will diffract into a different angle to produce an interference pattern at the output of the instrument, resulting in a superposition of fringes of different frequency and intensity. Herein lies the homodyne aspect of PHI: ***the interferometer essentially homodynes the entire input beam with itself keeping the zero-frequency fringe for the tuned λ_0 homodyne wavelength as reference.*** A combined pattern resulting from a multi-component spectrum is given by the summation of the individual monochromatic fringe patterns. Once it is imaged onto the detector, a Fourier transform of the interference pattern recovers the power spectrum of the input [10].

According to fringe frequency equations above, the *aliasing* problem occurs when $\phi=0$, in which case both $\lambda+\Delta\lambda$ and $\lambda-\Delta\lambda$ produce the same frequency and intensity distribution [10, 18]. This is easily addressed by slightly tilting one mirror perpendicular to the plane of interference. The $\phi \neq 0$ condition breaks the aliasing degeneracy by introducing $f_y \neq 0$. This *cross-tilt* introduces a fringe rotation that is counterclockwise or clockwise depending on whether the light is bluer or redder than the heterodyne wavelength. Thus, both the frequency and position angle of the fringes are indicators of the separation from λ_0.

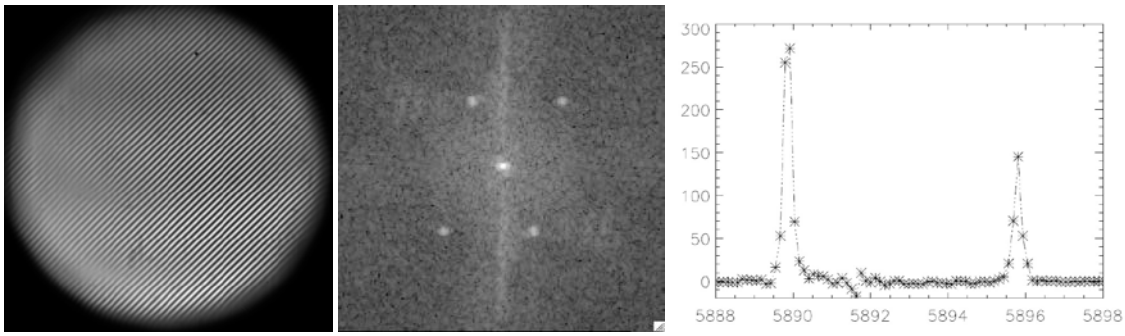

Figure 3. (Left) Fringe pattern from Na Hollow Cathode Lamp when the ground-based tunable reflective SHS built by Hosseini, et al. at Mt. Hamilton . The interferometer is tuned to the vicinity of the Na D lines at $\lambda_{\Delta 1}$= 5895.9 Å, $\lambda_{\Delta 2}$= 5889.9 Å. This image contains two set of fringe patterns each for one of the Na D lines. **(Middle)** The reduced power spectra shows both lines indicating both fringe pattern are present in the data. The top half of the 2D FFT is the repetition of the bottom half which an inverse wave-vector sign. **(Right)** The Na D lines' power spectra: the separation of $\Delta\lambda$=5.97 Å, indicates a resolving power of R~48000 which is same with the calculated R.

3.3 PHI Resolution and Field of View

The primary scientific advantage of a SHS, in either the reflective or Michelson design, is in its combination of high R and a large input FOV in a compact instrument. In a grating spectrograph, the spectral resolution is derived from both the dispersion relation at the detector and the width of the aperture in the wavelength direction. This convolution drives the R *lower* if the size of the instrument is reduced and/or its FOV is increased. Thus, the typical high ($R>10^5$; 3 km/s) resolution spectrograph has a very narrow FOV, is quite large, and is attached to a large telescope (e.g., the HST-STIS), while the typical low-resolution spectrograph on a remote probe (e.g., Voyager UVS or the New Horizons ALICE instrument) is compact, has a wide FOV, and *low* R (<1000; 300 km/s). The FOV in PHI is not convolved with spectral response and therefore, to a large degree, the spectral resolution is decoupled from the size of the area that is being sampled. This allows PHI to sample closer to the full theoretical resolving power of the grating which is defined by

$$R = \frac{\lambda_0}{\Delta\lambda} = 4mW_g G$$

$$FOV \approx \frac{2\pi}{R} \times \frac{W_g}{D_T}$$

where m is the diffraction order, W_g is the width of the beam on the grating, G is the grating groove density and D_T is the diameter of the coupling telescope. The data obtained from PHI is the integrated spectra over the FOV and if the angular extension of the target is smaller than the FOV, the background signal would add to the noise unnecessarily. For that reason it is of a value to match the size of the FOV to the angular size of the target of interest (in this case Mars' diameter from Earth' orbit).

3.4 PHI Spectral Bandpass

One of the main characteristics of SHS instruments that depending on the target of study can be considered as a limitation or advantage is the short spectral bandpass coverage. In SHS, the bandpass is defined by the highest resolved spatial fringe frequency number on the detector of a given format. The center of this bandpass is selected by the 'homodyne' wavelength (λ_0) (figure 2). The bandpass is determined by $\pm\Delta\lambda_B$ around λ_0. The theoretical limit of the bandpass is set by the Nyquist limit established by the number of pixels on the detector used. The practical bandpass limit is much less than this due to a

variety of factors such as the phasing of pixels and fringes, internal fringe distortions, or focus. The value of $\Delta\lambda_B$ for the normal incident light on the grating is given by

$$\Delta\lambda_B = \frac{\lambda_0}{\frac{Rk}{N} - 1}$$

where $\Delta\lambda_B$ is the half bandpass, R is the resolving power, k is the minimum number of pixels required to resolve one fringe (for the Nyquist limit: k=2), and N is the total number of pixels along the detector [10, 18]. At every observation the sampled bandpass is a small range (1-10 nm) and it is possible to tune to a wider bandpass by rotating the mirrors [10, 21]. In PHI, however, we are interested in observing CH_4 lines at 3.2 μm and the small bandpass, high spectral resolution and wide FOV with no moving parts is desirable. To demonstrate capability for planetary science, in this concept study, we targeted the spectral region between 3225 nm and 3235 nm for methane measurement because it contains molecular absorption lines of CH_4, as well as H_2O, and CO_2. The simultaneous measurement of all the three atmospheric components is highly desirable for this instrument concept. CH_4 and H_2O are of scientific interest and the CO_2 measurement can be used to infer accurate VMRs in the presence of single and multiple scattering by atmospheric aerosols.

3.5 PHI Calibration and Interface with Telescope

In principle PHI doesn't need to be coupled to a telescope to perform observations. The acceptance FOV of PHI is widest when coupled to no telescope or a siderostats with magnification of one. However when coupled to a telescope, the FOV reduces as discussed above. If PHI is coupled to a Cassegrain telescope the diffracted pattern of the secondary spider shadow would appear on top of the scientific interference fringe pattern. This effect has been extensively studied by Hosseini [9, 10]. There are software solutions to this issue but will introduce ambiguity in the data analysis [10]. For that reason PHI can be coupled to a small siderostat system or an off axis telescope with appropriate material and coating for the selected wavelength region.

4. PERCEIVED IMPACT TO STATE OF KNOWLEDGE

FTIR spectrometers like the MATMOS instrument on the ExoMars orbiter (descoped) are extremely sensitive for detecting a wide variety of gases including Mars methane. They collect high resolution spectra over a wide spectral range and provide survey capability at high sensitivities. PHI has a similar performance in addition can be made extremely compact in a reflective design and no moving parts, and therefore holds promise of wide applicability for a variety of observing opportunities in various space platforms. The impact on the state of knowledge will come in the increased opportunities and lower cost, mass, power of a miniature PHI instrument over the much larger instruments of similar sensitivity. Furthermore, because PHI has very high spectral resolution, it retains the spectral unambiguity of the FTIR technique in uniquely identifying molecules. Table 1 contains the comparison information between PHI and current stats of art instruments. The quantity of étendue is used to express the sensitivity of an optical instrument. However, for practical reasons in building new instruments, usually the goal is to optimize g*rasp* per cost. Grasp [10, 22] is defined as $G = \textit{Étendue} \times R$ and it is used to quantify the overall potential of an instrument considering the input aperture, *FOV*, and resolving power. One of the implementations of low grasp in common high *R* spectrometers is the steep trade-off between *R* and *FOV*; by increasing the *FOV* the instrument loses the *R* sensitivity.

The Planetary Homodyne Interferometer (PHI) studied here will have nearly identical sensitivity to Mars methane as FTIR spectrometers, except for recognizing the much more compact and simpler optomechanical design. Because of PHI's high étendue, we would be able observe the full disk of Mars for global Methane variations, if any, with small aperture telescopes at shorter time scales. From Mars' surface, PHI can observe the methane abundance dynamics at much less power, mass and cost. PHI targets methane lines and because it has a narrow spectral range it will have less undesirable signal contributing to multiplexing noise.

Table 1. Using only a small-aperture telescope, PHI can provide high spectral R capability at high FOV, étendue, and grasp compared to commonly used high-R spectrometers. This ability puts PHI among the high étendue instruments and in favorable group for grasp values. In calculating the étendue and grasp values, the FOV of the interferometers are assumed circular.

Instrument	Telescope	R	FOV	Étendue (m^2 $arcsec^2$)	Grasp x 10^5	Minimum detectable CH4/ref
PHI from Earth's orbit	0.5/off-axis	108,000	39 arcsec	440	475	0.7 ppbv
PHI on Mars surface	0.3m/off-axis	108,000	1 arcmin, 18 arcsec	440	475	0.06 ppbv
PHI orbiting Mars	0.05m/ Siderostat	108,000	26 arc min, 13 arcsec	440	475	0.06 ppbv
MATMOS FTIR	5cm/ExoMars	150,000	5 arcmin, 24 arcsec	206	310	0.05 ppbv/ Wennberg proposed
NIRSPEC	10m/NASA IRTF	3,7000	0.144x12 $arcsec^2$	135	50	8 ppbv /Mumma et al. upper limit
Planetary Fourier Spectrometer (PFS)	50cm/Mars Express	1,500	1.6 degree	1130	16	5 ppbv with thousands of spectra integrated over long periods
In situ TLS	SAM-MSL	27,000,000	*In situ* chamber	--------	--------	1 ppbv or 0.1 ppbv with enrichment

5. ACKNOWLEDGMENT

The research was carried out at the Jet Propulsion Laboratory, California Institute of Technology, under a contract with the National Aeronautics and Space Administration. Copyright will be transferred to SPIE.

REFERENCES

[1] C. R. Webster, et al.,, "Mars Methane Detection and Variability at Gale Crater," Science, 347, 415-417 (2015).
[2] C. Webster, et al., , "Low upper limit to methane abundance on Mars," Science, 342(6156), 355–357 (2013).
[3] M. J. Mumma, et al.,, "Strong release of methane on Mars in northern summer 2003," Science, 323(5917), 1041–1045 (2009).
[4] J. M. Harlander, Roesler, F. L. , Englert, C. R., Cardon, J. G., Conway, R. R., Brown, C. M., and Wimperis, J., "Robust monolithic ultraviolet interferometer for the SHIMMER instrument on STPSat-1," App. Opt., 42, 2829-2834 (2003).
[5] H. S. Stevens, Englert, C. R., Hervig, M., Petelina, S. V., Singer, W., and Nielsen, K.,, "The diurnal variation of polar mesospheric cloud frequency near 55ºN observed by SHIMMER," J. Atmos. Sol. Terr. Phys., 71, 401-407 (2009).
[6] J. M. Harlander, F. L. Roesler, and S. Chakrabarti, "Spatial heterodyne spectroscopy: a novel interferometric technique for the FUV." 1344, 120-131.
[7] S. Godlin Stephan, Chakrabarti, S., Vickers, J., Cook, T., and Cotton, D., "Interplanetary H Lyα observations from a sounding rocket," Ap. J., 559, 491-500 (2001).
[8] L. S. Rothman, et al., "HITRAN 2008 molecular spectroscopic database," J. Quant. Spectrosc. Radiat. Transfer, 110, 533–572 (2009).
[9] S. Hosseini, Harris, Walter "First calibration and visible wavelength observations of Khayyam, a tunable spatial heterodyne spectroscopy (SHS)," Proc. SPIE 9147, Ground-based and Airborne Instrumentation for Astronomy, 91478L, 9 (2014).
[10] S. S. Hosseini, [Tunable Reflective Spatial Heterodyne Spectrometer: A Technique for High Resolving Power, Wide Field Of View Observation Of Diffuse Emission Line Sources] University of California Davis, (2015).

[11] J. M. Harlander, [Spatial Heterodyne Spectroscopy: Interferometric Performance at any Wavelength Without Scanning.] University of Wisconsin-Madison, (1991).

[12] T. Dohi, Suzuki, T., “Attainment of High Resolution Holographic Fourier Transform Spectroscopy,” Applied Optics, 10, (1971).

[13] C. R. Englert, M. H. Stevens, D. E. Siskind *et al.*, “Spatial Heterodyne Imager for Mesospheric Radicals on STPSat-1,” Journal of Geophysical Research-Atmospheres, 115, (2010).

[14] M. Florjanczyk, P. Cheben, S. Janz *et al.*, "Development of a slab waveguide spatial heterodyne spectrometer for remote sensing." 7594, 75940R.

[15] W. Harris, F. Roesler, L. Ben-Jaffel *et al.*, “Applications of spatial heterodyne spectroscopy for remote sensing of diffuse UV-vis emission line sources in the solar system,” Journal of Electron Spectroscopy and Related Phenomena, 144, 973-977 (2005).

[16] S. Chakrabarti, Cotton, Daniel M., Vickers, James S., Bush, Brett C., “Self-compensating, all-reflection interferometer,” Applied Optics, 33(13), (1994).

[17] B. Douglas, Melis, (1990).

[18] S. Hosseini, Gong, Aaron, Ruth, Dustin, Baldis, Hector A., Harris, Walter, “Tunable spatial heterodyne spectroscopy (TSHS): a new technique for broadband visible interferometry,” Proc. SPIE, 7734(77343J), 12 (2010).

[19] S. Hosseini, [Tunable Reflective Spatial Heterodyne Spectrometer: A Technique for High Resolving Power, Wide Field of View Observation of Diffuse Emission Line Sources] University of California Davis, (2015).

[20] J. Harlander, Reynolds, R.J., Roesler, F. L., “Spatial heterodyne spectroscopy for the exploration of diffuse interstellar emission lines at far-ultraviolet wavelengths,” Astrophysical Journal(396), 730-740 (1992).

[21] O. R. Dawson, Harris, W. M., “Tunable, all-reflective spatial heterodyne spectrometer for broadband spectral line studies in the visible and near-ultraviolet,” Applied Optics, 48(21), 4227-4238 (2009).

[22] R. G. Bingham, “Grating spectrometers and spectrographs re-examined,” Royal Astronomical Society, Quarterly Journal,, 20, (1979).